

Chapter 10

Apparatus: Orthotropic Oven and Zeeman Slower

10.1 Introduction

A method of producing slow francium atoms for capture into a MOT from a beam is to slow the atoms with a counter propagating laser beam while they pass through a magnetic field that changes along the beam path so as to keep the slowing atoms in resonance with the laser (Zeeman slower). High flux and high brightness Zeeman slowers have been built, but because they used stable alkali atoms, they did not need also to be high efficiency. Because beams of alkali atoms can be slowed, deflected, focused and dissipatively cooled in all three directions, it is as a matter of accelerator physics possible to slow most of the alkali atoms in a thermal beam and capture them into a MOT. The practical limitations are size and laser power—which is to say size, effort, and money.

The general problem to be overcome is the source divergence and the first problem to overcome is the large divergence of a thermal source. This has been done by Slowe, Vernac, and Hau [SVH05] by using a candlestick source for Rb atoms that form a liquid reservoir, achieving a 0.1 radian half-angle cone, and by Dinneen, Ghiorso, and Gould [DGG96] using an orthotropic oven for francium, achieving a ± 0.15 radian full width distribution. As there is not enough francium to form a reservoir we will use an orthotropic oven (Section 10.2).

Next is to reduce the angular divergence from the source before the beam gets so large as to pose

size problems. This is done (Fig. 10.1) by multiple stages of transverse cooling (Section 10.3). The common problem in Zeeman slowers is then the growth in the normalized phase space: the increase in relative divergence as the longitudinal velocity is reduced but the transverse velocity remains. This will be solved by interrupting the deceleration at about 60 m/s. At this point all atoms that left the oven traveling 60 m/s or higher are now traveling 60 m/s—only a few percent of atoms that left the oven traveling less than 60 m/s are present in the beam (Fig. 10.5). This single velocity beam is allowed to expand, is then focused by a sextupole magnet and at the focus is laser cooled in both transverse directions. The beam is then further slowed and captured into the collection MOT. If necessary, a final focus to match the francium beam to the MOT can be added. The resulting apparatus (Fig. 10.1) is long and may require over a Watt of laser power, but such an apparatus appears capable of accepting over half of the atoms, initially free inside the oven, into a MOT with a capture velocity of as low as ten m/s.

10.2 Orthotropic Oven

10.2.1 Principle of Operation

The orthotropic oven [DGG96] for use with francium works on the principle that, in a beam from an effusive source, the low divergence atoms originate from the region directly behind the exit aperture.

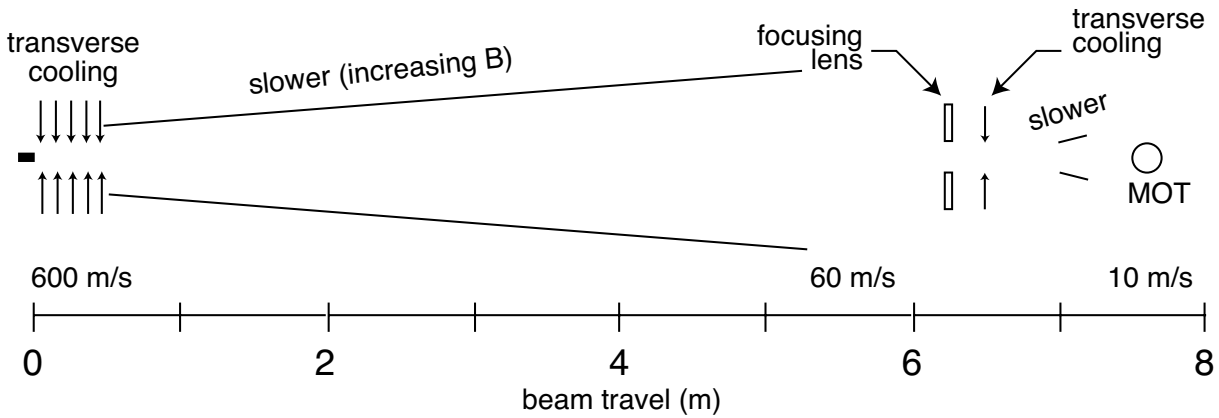


Figure 10.1: Schematic diagram of the slowing apparatus. The orthotropic oven (dark rectangle at the extreme left) operates at 1220 K and produces a beam of ^{221}Fr with a maximum divergence of 0.030 radians. In the francium beam, 88.8% of the atoms have velocity of 600 m/s or less and therefore transverse velocities of 18 m/s or less. It is these atoms that are cooled and slowed. The atoms are first transversely cooled using lasers detuned by three, two and then one linewidth to reduce the transverse velocity to ≈ 0.1 m/s. The francium beam, which at this point has grown to about ± 5 mm width, enters the first slower section. It is slowed to 60 m/s and, due to heating, increases its transverse velocity to about 1.25 m/s. At 60 m/s its divergence is now 0.021 radians. The beam is allowed to drift and is then focused by a permanent-magnet sextupole or by a two-dimensional MOT with a focal length of 30 cm. This brings the beam to a focus with a transverse velocity of about 6 m/s. At this point the francium is laser cooled back to about 0.1 m/s. It then enters a second slower which reduces it velocity to 10 m/s. From there it can either directly enter the MOT or be further focused and transported.

The orthotropic oven then reduces the probability that atoms from other locations will exit the aperture by causing atoms at other surface locations to be ionized and attracted back to a neutralizer di-

rectly behind the exit aperture (Fig. 10.2). Francium, with ionization potential of $I = 4.073$ eV, is surface ionized by the oven walls made from, or coated with, a high work function metal such as platinum (work function $\Phi = 5.65$ eV) so that atoms hitting the walls have a high probability of evaporating as ions. The ions are then electrostatically attracted to a neutralizer made from a low work function metal such as yttrium ($\Phi = 3.4$ eV) situated directly behind the exit aperture. The francium evaporates from the neutralizer and either passes through the exit aperture or strikes the walls and is again ionized and collected by the neutralizer.

The ratio of ions (i_+) to neutral atoms (i_0) evaporated from the oven walls is given by

$$\frac{i_+}{i_0} = \frac{1}{2} \exp \left[\frac{1.602 \times 10^{-19}(\Phi - I)}{kT} \right], \quad (10.1)$$

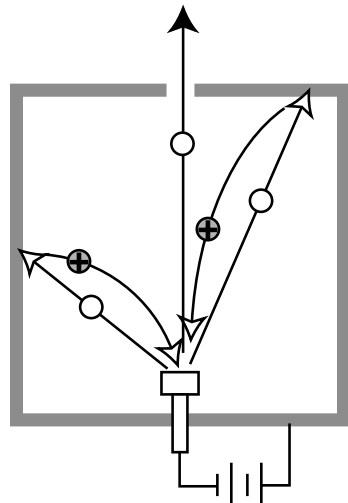


Figure 10.2: Schematic of the Fr orthotropic oven. The filled circles are Fr^+ ions and open circles are neutral Fr atoms.

where $k = 1.38 \times 10^{-23}$ J/K. For a platinum surface oven wall at 1220 K, as used in Ref. [DGG96], we have $i_+/i_0 = 1.6 \times 10^6$; and for francium released from the yttrium neutralizer we have $i_+/i_0 = 8.3 \times$

Table 10.1: Quantities Used in this Section

Quantity	Symbol	Value and Units
Width of orthotropic oven exit slit	w_{exit}	variable
Width of orthotropic oven neutralizer	$w_{\text{neutralizer}}$	variable
Distance between neutralizer and exit	l_{ne}	variable
Full intensity of a francium beam	I_{full}	variable
Francium beam intensity at v to $v + dv$	I_{beam}	variable
Mass of ^{211}Fr	M	$3.53 \times 10^{25} \text{ kG}$
Orthotropic oven temperature	T	1220 K
Boltzmann Constant	k_B	$1.38 \times 10^{-23} \text{ J/K}$
Most probable velocity in ^{211}Fr beam	$v_k = \sqrt{2kT/m}$	310 m/s
Optical wavelength $7P_{3/2} \leftrightarrow 7S_{1/2}$	λ	718 nm
Wave number	$k = 2\pi/\lambda$	$8.75 \times 10^6 \text{ m}^{-1}$
Acceleration by laser light	a	variable (typ. 10^4 m/s^2)
Lifetime of $7P_{3/2}$ state	τ	$2.1 \times 10^{-8} \text{ s}$
Linewidth of $7P_{3/2} \leftrightarrow 7S_{1/2}$	$\Gamma = 1/\tau$	$4.76 \times 10^7 \text{ s}^{-1}$
Laser detuning	Δ	variable (Hz)
Plank's constant	h	$6.625 \times 10^{-34} \text{ Js}$
Plank's constant/ 2π	\hbar	$1.05 \times 10^{-34} \text{ Js}$
Saturation intensity	$I_0 = \pi h c / 3\lambda^3 \tau$	26.7 W/m^2
Ratio of laser power to I_0	s	variable
Transverse velocity	v_{\perp}	variable (m/s)
Longitudinal velocity	v_{\parallel}	variable (m/s)
Doppler cooling limit	v_D	0.089 m/s
Laser – atomic beam angle to normal	θ	variable
Magnetic field (in Zeeman slower)	$B(z)$	variable (T)
Bohr magneton	μ_B	$927 \times 10^{-26} \text{ J/T}$
Bohr magneton	μ_B	$1.4 \times 10^{10} \text{ Hz/T}$
g factor for $7P_{3/2}$ state	g_J'	$4/3$
g factor for $7S_{1/2}$ state	g_J	2
Focal length of sextupole or MOT	f	30 cm
Length of permanent magnet sextupole	L	6 cm
Radius of sextupole magnet gap	ρ	3 cm
Inhomogeneous magnetic field	$\partial^2 B / \partial \rho^2$	0.37 T/cm^2

10^{-4} (except that the electric field keeps the ions at the neutralizer until they evaporate as neutral atoms).

10.2.2 Reducing Divergence

The first orthotropic oven (Ref. [DGG96]) produced a francium beam with ± 0.15 radian divergence (Fig. 10.3). Although thermal atomic beams, with divergences of 0.1 radian, have been laser cooled in both transverse directions [Hoo93, HDV⁺96, SVH05], it would be better to use an oven with

a smaller divergence because, even as the divergent beam of atoms is being cooled, the atoms are spreading transversely. It is also easier and cheaper to machine metal and drill holes to make ovens than to assemble and align large quantities of lasers and optics.

The original orthotropic oven had a 3 mm diameter neutralizer and a 5 mm diameter exit aperture spaced 23 mm from the neutralizer. As Fig. 10.3 shows, the umbra covers a small portion of the distribution (about 0.045 radians) while the penum-

Table 10.2: ^{211}Fr ancium Beams from an Orthotropic Oven

neutralizer diameter (mm)	exit aperture (mm)	l_{ne} (mm)	umbra (radians)	penumbra (radians)	escape probability per attempt
3.0	5	23	0.043	0.174	5.9×10^{-3}
3.0	10	93	0.038	0.070	1.5×10^{-3}
3.0	10	220	0.016	0.030	2.6×10^{-4}
1.5	5	47	0.037	0.069	1.4×10^{-3}
1.5	5	110	0.016	0.030	2.6×10^{-4}
1.5	10	82	0.052	0.070	1.9×10^{-3}
1.5	10	190	0.022	0.030	3.5×10^{-4}

bra covers most of the ± 0.15 radians. The angular one dimensional size of the umbra θ_u and of the penumbra θ_p of a *rectangular slit* are, from Ramsey [Ram56],

$$\theta_u = \frac{1}{2} \left| \frac{w_{\text{exit}} - w_{\text{neutralizer}}}{l_{ne}} \right| \quad (10.2)$$

$$\theta_p = \frac{1}{2} \left| \frac{w_{\text{exit}} + w_{\text{neutralizer}}}{l_{ne}} \right| \quad (10.3)$$

where w_{exit} is the width of the exit slit, $w_{\text{neutralizer}}$ is the width of the neutralizer, l_{ne} is the neutralizer to exit hole distance, and we have assumed that the distance to the observation point is very large compared to the collimator width. Because

the aperture in the orthotropic oven is circular, the penumbra is slightly smaller (0.15 radians) than a rectangle with sides equal to the aperture diameter of 0.17 radians.

The goal here is to both decrease the angular divergence of the beam and to make the size of the penumbra closer to that of the umbra. The latter is accomplished by having a large ratio of exit aperture diameter to neutralizer diameter. However we do not yet know how much smaller the neutralizer can be made than the three-mm diameter neutralizer in Ref. [DGG96]. In Table 10.2 several options for ovens with 30 milliradian and 70 milliradian divergences are compared with the first orthotropic oven.

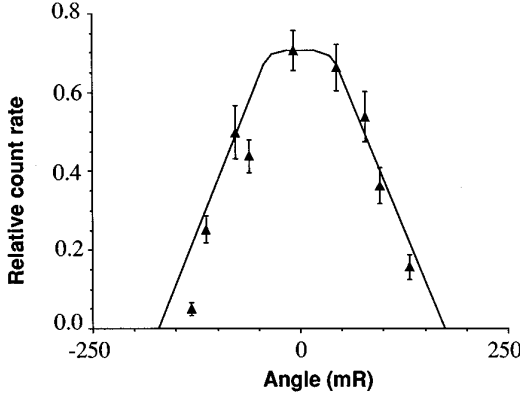


Figure 10.3: Measured angular distribution of a ^{221}Fr atom beam. The central region of constant intensity is the umbra and the larger region of changing intensity is the penumbra.

10.2.3 Orthotropic Oven Efficiency

In the only orthotropic oven model measured, the probability that a francium atom produced inside the oven would escape into the collimated beam was 0.15. That however was largely due to the ^{221}Fr being produced by alpha decay of ^{225}Ac in which the francium daughter recoils with an energy of 105 keV and buries itself in either the oven wall (platinum) or the radioactive source substrate (nickel). That probably set a probability ceiling of 0.5. In Ref. [DGG96], measurements on heated foils showed that at 1220 K, release fractions of about 0.25 and 0.35 could be obtained for francium, recoiled in air so that the francium landed with much less energy, escaping platinum and nickel foils respectively. And it was observed that, at 1220 K,

the oven efficiency was still increasing with increasing temperature. This points to losses associated with the introduction of the francium into the oven as being the largest inefficiency. This type of loss is not expected to change with larger oven dimensions.

A remaining question is to what extent reducing the beam divergence might reduce the efficiency of the oven. With smaller beam divergence it takes more tries for the francium atom to pass through the exit aperture requiring the francium atoms to spend more time in the oven where they may radioactively decay. Each failed attempt to escape the oven involves a round trip between the neutralizer and the oven wall, hence each attempt takes twice the average transit time between the neutralizer and the wall plus the sticking time on the wall and the sticking time on the neutralizer. Scheer et al. [SKM71] have measured surface lifetimes for ionization of alkali metals by molybdenum, and Gladyszewski has measured ionization and sticking times on rhenium [Gta94]. From these we infer an average time of 0.3 ms for the sticking times, both on the oven walls and on the neutralizer, at 1220 K. The sticking times increase rapidly with decreasing temperature so it is unlikely that the oven could be cooler than 1200 K without reducing overall efficiency. Table 10.2 shows, for different oven dimensions, the escape probability per attempt. Even for the largest ovens with the most attempts per escape, the decay fraction for ^{211}Fr ($t_{1/2} = 3.1\text{ min}$) is only a few percent.

In an oven with more cycles, more francium might be lost because it is chemically reacting with the (alumina) insulator holding the neutralizer. This seems unlikely because Fr_2O should decompose at 700 K. The Fr^+ may not readily neutralize when it lands on the insulator due to the electronegativity of the alumina, in which case a more complicated mechanical design can reduce the alumina surface area readily seen by the francium ions. The 100 eV kinetic energy acquired by the ion may cause the release from the neutralizer to take longer than 0.3 ms, a problem that can be corrected with higher oven temperature or lower voltage or both.

10.2.4 Loading the Orthotropic Oven

To load ^{225}Ac into the orthotropic oven it is only necessary to drop in a small piece of nickel or platinum ribbon (or any high work function metal) on which ^{225}Ac has been deposited, as was done in Ref. [DGG96]. To load francium from an ion beam, such as a 30 kV Fr^+ beam at TRIUMF, we suggest the following method: the beamline is connected to the orthotropic oven through a transport tube. The last portion of beam transport tube is coated with a high work-function metal, heated, and biased with respect to the neutralizer to keep ions from returning (Fig. 10.4). The tube is also positioned so that, looking from the neutralizer, there is no direct line of sight down the tube.

At 30 kV, the francium will travel into the oven wall and will need to diffuse out. Melconian et al. [MTG⁺04] have studied the diffusion of ^{37}K from heated metal foils after ^{37}K implantation at 12 keV. They find (Fig. 2 of Ref. [MTG⁺04]) that at 1200 K, the release fraction of ^{37}K is 0.35 from Pt and 0.6 from Ni. The orthotropic oven [DGG96] had an overall efficiency of 0.15, and platinum and nickel foils, heated to 1220 K, had release fractions of 0.25 and 0.35, respectively: pleasingly similar.

Using the oven efficiency of 0.15, scaling the for-

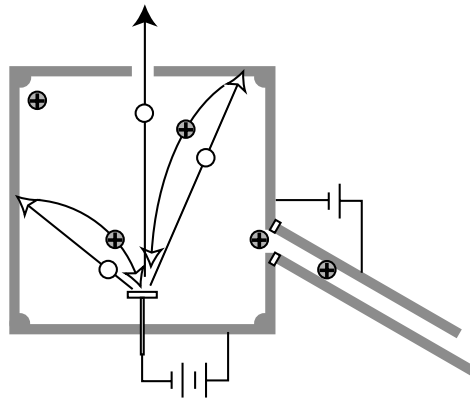


Figure 10.4: Schematic of the Fr orthotropic oven with a 30 keV beam of ^{211}Fr ions from TRIUMF entering from the right. The last several cm of beam transport tube is coated with a high work-function metal, heated, and slightly biased to keep ions from returning.

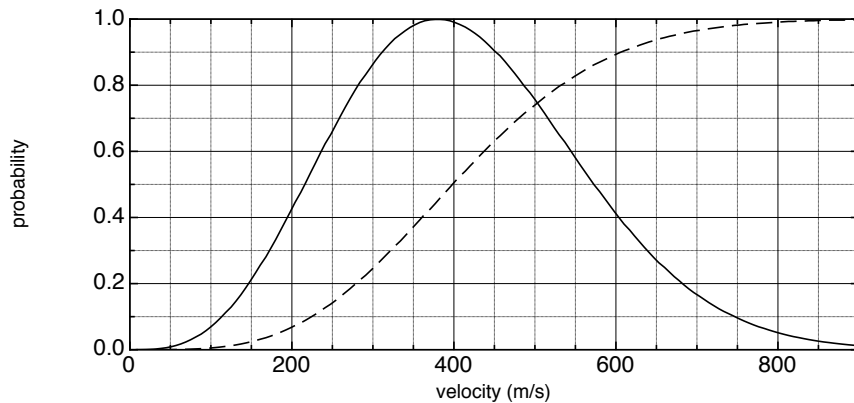


Figure 10.5: Normalized velocity distribution of ^{211}Fr atoms in a beam formed at 1220 K (solid line) and the cumulative probability of finding a ^{211}Fr atom at less than or equal to that velocity (broken line).

mulas in Melconian et al. [MTG⁺04], and extrapolating ion range from Powers and Whaling [PW62] gives 0.4 as a rough estimate of a release efficiency at 1220 K for 30 keV francium implanted in platinum. At lower implant energies, the release fractions increase and may reach 0.8 or more at a few keV [MTG⁺04]. As the Fr^+ beam from TRIUMF has only a 10 mm mr divergence, it should be possible to slow the beam (such as by biasing the orthotropic oven) without losing beam due to normalized emittance growth. This would considerably increase the release fraction.

Using a two-stage oven with a loading section and an orthotropic section may also improve loading efficiency if the loading section is made from, or coated with, more release-friendly metals such as Zr, V, Y, or Hf; or operated at a higher temperature; or both [MTG⁺04]: release efficiencies of 0.8 might be obtained. A small bias potential would again prevent ions in the orthotropic section from reentering the collection section. Again, this device can be prototyped using ^{221}Fr generated from ^{225}Ac .

10.2.5 Longitudinal and Transverse Velocity of a Thermal Beam

The flux of atoms in a thermal beam is proportional to the atom's velocity because there are more atoms per second passing a fixed point if the atoms are moving faster. The velocity distribution is thus

modified from a Maxwell-Boltzmann distribution by an extra factor [Ram56, MvdS99d] of velocity, v , and is

$$I_{\text{beam}}(v) = \frac{2I_{\text{full}}}{v_k} v_k^3 \exp\left[-\frac{v^2}{v_k^2}\right]. \quad (10.4)$$

Here I_{full} is the full beam intensity, $I_{\text{beam}}(v)$ is the beam intensity of atoms from velocities v to $v + dv$, and $v_k = \sqrt{2k_B T/M}$ is the most probable velocity, and $k_B = 1.38 \times 10^{-23} \text{ J/K}$ is the Boltzmann constant, T is the temperature, and $M = 3.5 \times 10^{-25} \text{ kg}$ is the mass of ^{211}Fr . At $T = 1220 \text{ K}$ we have $v_k = 310 \text{ m/s}$.

The length of the slower and the length of the transverse cooling section depend on the highest velocity atom that is to be slowed. If we choose 600 m/s then, as shown in Fig. 10.5, we find that 88.8% of the francium atoms in the beam can in principle be cooled and slowed. The maximum transverse velocity will, for ± 0.030 radians, be $v_\perp = 18 \text{ m/s}$. (We neglect the longitudinal velocity difference between an atom at 0.030 radians and 0 radians.)

10.3 Transverse Cooling

10.3.1 Acceleration and Cooling by Counter-Propagating Red-Detuned Laser Beams

The transverse velocity of a thermal beam of neutral

atoms with divergences up to about 0.10 radians can be rapidly reduced to near zero by laser cooling to produce a collimated beam with a 1 or 2 cm diameter [AVK90, Hoo93, HDV⁺96, SVH05], even for atoms traveling 600 m/s [Hoo93]. An atom in a standing wave of (slightly) red-detuned laser light will, if traveling with velocity v in the direction of the laser beam, see the light Doppler shifted towards resonance by a frequency $\Delta\nu = kv$, where $k = 2\pi/\lambda$ is the wave number and λ the wavelength (718 nm for the Fr $7S_{1/2} \leftrightarrow 7P_{3/2}$ transition). Consequently the atom will scatter more photons from this laser beam than from the opposite, red shifted beam, and thus experience a net radiation force.

Francium, being more massive than other alkali atoms, experiences a smaller acceleration for the same force and will require more transitions and a longer time to slow and cool. Starting with a francium beam from the orthotropic oven with a divergence of ± 0.030 radians, rather than ± 0.1 radians or even ± 0.070 radians, helps constrain the size and cost of the apparatus.

The acceleration a for an atom of mass M with transverse velocity v_\perp collinear to the laser, is

$$a = \frac{\hbar k \Gamma}{2M} \frac{s}{1 + s + [2(kv_\perp + \Delta/\Gamma)]^2}. \quad (10.5)$$

Here $\Gamma = 1/\tau = 4.76 \times 10^7 \text{ s}^{-1}$ is the linewidth of the francium $7P_{3/2} \leftrightarrow 7S_{1/2}$ transition of lifetime τ , and $s = I/I_0$ is the saturation parameter, I is the laser intensity and I_0 is the saturation intensity, and Δ is the laser detuning, usually given in units of Γ . The saturation intensity is given [MvdS99d] by $I_0 = \pi hc/3\lambda^3\tau = 26.7 \text{ W/m}^2$ (2.67 mW/cm^2).

Figure 10.6 shows the acceleration available for cooling ^{211}Fr by counter-propagating laser beams, red detuned by one-half linewidth. Note that because of the atom's linewidth, there is still some acceleration from the laser beam that is in the direction of the atom's motion. The fact that the acceleration becomes small at small velocities has only a small effect on the final displacement because those atoms already have small transverse velocities. It does make the slowing time longer and

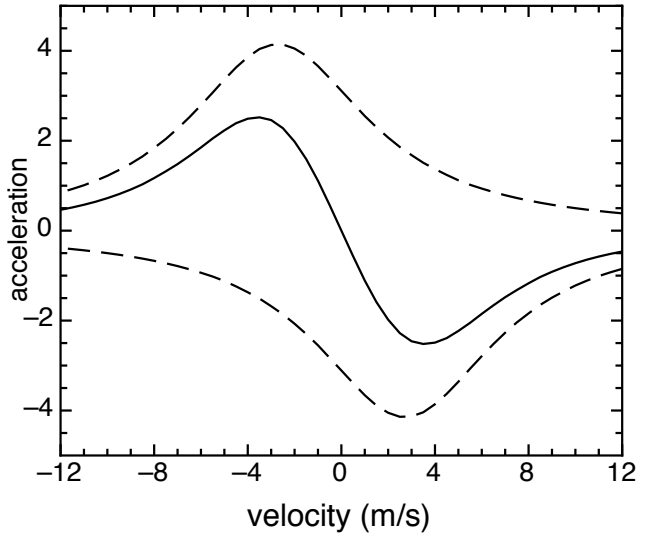


Figure 10.6: Acceleration of ^{211}Fr atoms in units of 10^4 m s^{-2} as a function of the atom's velocity component, collinear with two counter propagating laser beams of intensity $s = 2$ and red detuned by $\Gamma/2$. The broken lines shows the acceleration from each of the two laser beams and the solid line is the resultant.

hence increases the beam's downstream travel and the length of the slowing section. Other than requiring laser power over a greater area, this is not an issue for the experiment.

Because the transitions also heat the beam, one limit on laser cooling is the equilibrium reached between heating and cooling, corresponding to a velocity [AVK90]

$$v_D = \sqrt{\frac{\hbar \Gamma M}{6} \left(\frac{2|\Delta|}{\Gamma} + \frac{\Gamma}{2|\Delta|} \right)}, \quad (10.6)$$

where $v_D = 0.089 \approx 0.1 \text{ m/s}$ for ^{221}Fr .

The acceleration of a francium atom in two counter-propagating red-detuned ($\Delta = -\Gamma/2$) laser beams, calculated from Eq. 10.5, is shown in Fig. 10.6. A francium atom will be slowed from $v_\perp = 5 \text{ m/s}$ to $v_\perp \approx 0.1 \text{ m/s}$ in $3.7 \times 10^{-4} \text{ s}$, during which time it will have traveled about 0.6 mm transversely. If the atom is traveling longitudinally at $v_{||} = 600 \text{ m/s}$, then it will have traveled about 0.22 m downstream. This arrangement is commonly used for brightening beams in both transverse directions. However, the

range of velocities that can be addressed is limited: in particular it does not produce any appreciable acceleration for atoms with $v_{\perp} = 18 \text{ m/s}$.

10.3.2 Transverse Cooling of ^{211}Fr with Divergences to 0.030 Radians

The (transverse) velocity range over which the atoms can be cooled can be increased by using higher power and the range of cooling can be shifted to higher velocity by larger laser detuning and/or by changing the angle between the laser and the beam of atoms. We examine each of these possibilities.

Laser Power

Increasing the laser power will increase the range of velocities that experience high acceleration and can also increase the acceleration. However the increase in acceleration is limited beyond $s = 2$ where the acceleration rises slowly with power (Eq. 10.5 and Fig. 10.7). The greater range is most helpful at

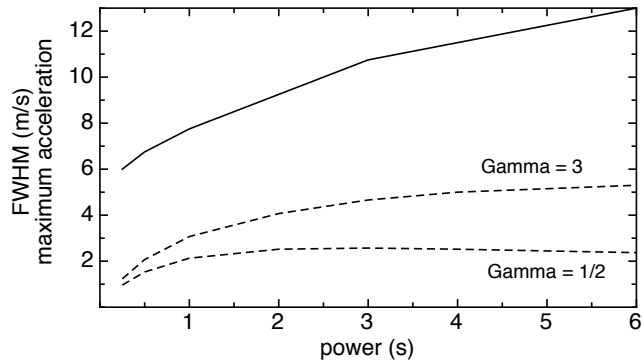


Figure 10.7: Solid line shows the FWHM range of initial velocity in m/s over which atoms are accelerated by at least 50% of their peak acceleration as a function of laser power in units of saturation parameter s . Broken lines show the maximum acceleration of ^{211}Fr in units of 10^4 m s^{-2} as a function of laser power for laser detunings Γ of three linewidths and of Γ of one-half linewidth.

large laser detuning, where the contribution to acceleration from the laser beam in the direction of v_{\perp} is small, but at small detuning used near $v_{\perp} = 0$, high power is actually counterproductive.

Multiple Cooling Sections Using Laser Beams with Different Detuning

If we start with a laser beam, red detuned by three linewidths, it will slow ^{211}Fr atoms from $v_{\perp} = 18 \text{ m/s}$ to about 13 m/s . Following that by laser beams detuned by two linewidths, those atoms will be slowed from $v_{\perp} = 13 \text{ m/s}$ to about 8 m/s . After that, laser beams detuned by one linewidth will decelerate the atoms to about 0.1 m/s . The acceleration from these lasers is shown in Fig 10.8. The acceleration and hence the cooling efficiency drops for small transverse velocities so that it takes much longer to cool from $v_{\perp} = 1 \text{ m/s}$ to $v_{\perp} = 0.5 \text{ m/s}$ than from 18 m/s to 17.5 m/s . However at small v_{\perp} the beam is no longer rapidly diverging so the increased cooling time does not result in appreciable beam broadening (Fig. 10.9).

To show how this would actually work, we calculate the francium atom's transverse velocity (v_{\perp}) and transverse displacement as a function of travel downstream from the orthotropic oven. We use the most extreme case of a longitudinal veloc-

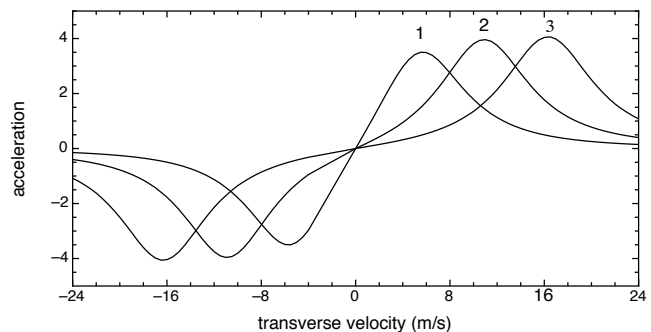


Figure 10.8: Acceleration of ^{211}Fr atoms in units of 10^4 m s^{-2} as a function of the atom's velocity component that is collinear with two counter propagating laser beams of intensity $s = 2$ and red detuned by three linewidths, two linewidths, and one linewidth ($\Delta/\Gamma = 3, 2, \text{ and } 1$).

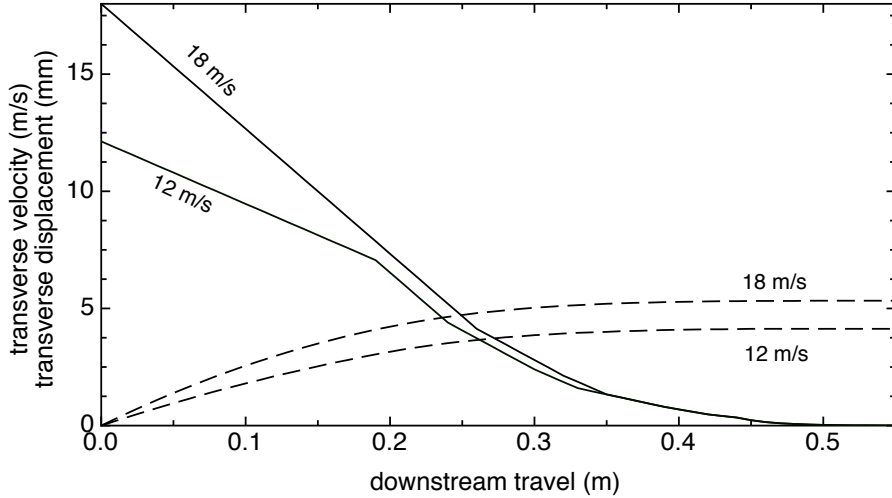


Figure 10.9: Decrease in transverse velocity v_{\perp} in m/s (solid lines) as a function of distance downstream from the orthotropic oven, and the transverse displacement in mm (broken lines) from the beam divergence, both for ^{211}Fr atoms with initial transverse velocities of $v_{\perp} = 18 \text{ m/s}$ and $v_{\perp} = 12 \text{ m/s}$ and longitudinal velocity of 600 m/s. The changes in the slope of velocity versus downstream travel are at the transition between regions of different laser detuning.

ity $v_{\parallel} = 600 \text{ m/s}$ and starting transverse velocity of $v_{\perp} = 18 \text{ m/s}$ (corresponding to a divergence of 0.030 radians).

The results, shown in Fig. 10.9, indicate that the atoms can be cooled in 0.5 m of longitudinal travel and emerge with a spread in transverse position of less than $\pm 5 \text{ mm}$. Although the needed cooling section is long (a half-meter of length needs to be illuminated with laser beams in both transverse directions), the francium beam that emerges has acceptable size and little divergence and so can be readily transported without loss. This represents only an example, with no attempt to optimize the cooling, either in terms of beam travel or spread. Using more than three detuning sections and higher laser power at the largest detuning may be advantageous.

One way to obtain the necessary laser beams is to split a primary beam into three beams and pass each through an acousto-optic modulator to obtain beams with detuning of $\Delta/\Gamma = 1$, $\Delta/\Gamma = 2$, and $\Delta/\Gamma = 3$ (detunings of 47.6 MHz, 95.2 MHz, and 143 MHz, respectively). These three beams are then each either split twice to make 12 counter propagating beams for the two transverse directions, or split once to make beams for the two transverse

directions and the counter propagating beams obtained by reflection from mirrors. As a final step each beam is expanded.

In our example the $\Delta/\Gamma = 3$ -detuned laser beams would need to be 9 cm long, the $\Delta/\Gamma = 2$ -detuned laser beams 8 cm long, and the $\Delta/\Gamma = 1$ -detuned laser beams 35 cm long. If the laser beams are one cm high, then the laser power needed for $S = 2$ is 1060 mW for 12 beams and 530 mW for six beams reflected.

In this example, we assumed that each laser detuned beam was applied sequentially. However, if in the first slowing section, the $\Gamma = 2$ and the $\Gamma = 1$ detuned laser beams are added to the $\Gamma = 3$ detuned beams, and in the second slowing section, the $\Gamma = 1$ detuned beam is added to the $\Gamma = 2$ detuned beam, then atoms with smaller transverse velocities will begin slowing immediately in the first section and continue slowing in the second section. This will result in a francium beam with more of the atoms concentrated towards the center and only a shell of the fastest atoms with the largest initial divergences at the largest distances from the centerline.

Having only the fastest atoms at the largest distances from the centerline may make it easier to

focus the beam downstream and may make it possible to focus the beam before it enters the slower¹. Future consideration of this point may be taken up in a more complete analysis.

Multiple Cooling Sections Using Doppler-Shifted Laser Beams

Rather than detune the laser, the capture range can be shifted by orienting the laser beam to point slightly downstream from the normal. This Doppler shifts the atoms with larger v_{\perp} into resonance. Eq. 10.5 then becomes

$$a = \frac{\hbar k \Gamma}{2m} \frac{s}{1 + s + [2(-kv_{\parallel}\theta + kv + \Delta/\Gamma)]^2}. \quad (10.7)$$

Here θ is the angle to the normal of the atomic beam, and the resulting Doppler shift is $kv_{\parallel}\theta$, where v_{\parallel} is the longitudinal velocity of the atom.

This is shown in Fig. 10.10 for laser beams at discrete angles to the francium beam of 0.024, 0.016, 0.008, and 0 radians respectively. The resulting transverse velocity and transverse displacement downstream is then similar (a little better) than described for the laser detuning method in Fig. 10.9. Changing the angle between the laser beam and francium beam can be done continuously by using convergent light (Aspect et al. [AVK90] such as by passing a parallel laser beam through a convex lens, or by reflecting a laser beam between two flat mirrors at a slight angle to each other as was done by Hoogerland et al. [Hoo93, HDV⁺96], and by Slowe, Vernac, and Hu [SVH05], so that after each reflection the laser beam becomes closer to the normal.

¹If one attempts to focus a beam with a large velocity spread, as is the case in a thermal beam, the slowest atoms will focus at shorter distances and be diverging where the fastest atoms focus. Here however, only the fastest atoms should be at the largest displacement and experience a large restoring force. Slower atoms still focus closer, but having only a small initial displacement, are little affected by the focusing element. This has some similarity to alternating gradient focusing.

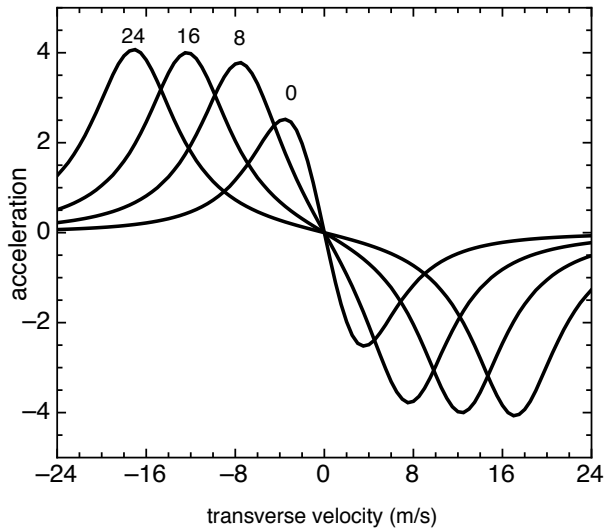


Figure 10.10: Acceleration of ^{211}Fr atoms in units of 10^4 m s^{-2} as a function of the atom's transverse velocity, v_{\perp} (m/s) produced by two counter propagating laser beams of saturation $s = 2$, detuned by $\Delta/\Gamma = 1/2$, and oriented at angles of 0.024, 0.016, 0.008 and 0 radians labeled 24, 16, 8, and 0, respectively.

Using a single laser beam at a variable angle to the francium beam is simpler than discrete laser beams of different detunings, and requires much less laser power if nearly parallel mirrors are used. However effects such as changes in intensity of the laser across the atomic beam [AVK90], defocusing of slow atoms [SVH05], and other possible nonlinear effects need to be well understood, preferably through simulation and modeling.

10.3.3 Transverse Cooling of ^{211}Fr with Divergences to 0.075 Radians

Our understanding of the workings of the orthotropic oven is at a level that makes it likely that a new prototype will be able to efficiently produce francium beams with 0.030 radians divergence. However, it is still worth considering if francium beams with significantly larger divergences can be cooled and transported through a slower. We therefore calculated, for $v_{\parallel} = 600 \text{ m/s}$, transverse displacement and longitudinal slowing distance

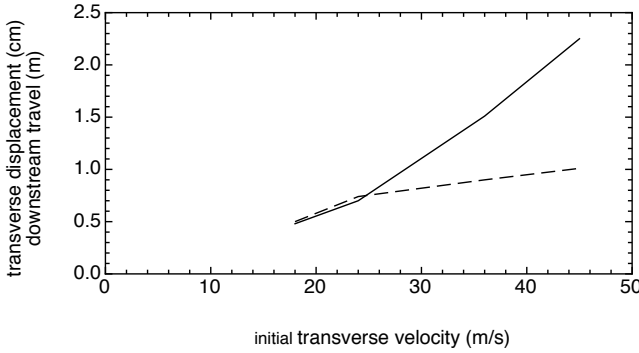


Figure 10.11: Distance (meters) needed to transversely cool (broken line) and final transverse displacement in mm (solid line) as a function of initial transverse velocity for francium atoms with longitudinal velocity of 600 m/s. In the calculation, as many as eight sections of slowing with different detuning were used. For detuning $\Delta/\Gamma > 1$ the power density was increased from $s = 2$ to $s = 4$.

for initial transverse velocities of 24 m/s, 36 m/s, and 45 m/s, corresponding to initial francium beam divergences of 0.045, 0.060, and 0.075 radians, respectively. A divergence of 0.075 radians is a factor of two smaller than the observed performance of the first model orthotropic oven [DGG96].

The results, calculated using Eq. 10.5 with $s = 4$ and detunings of up to $\Gamma/\Delta = 8$, are shown in Fig. 10.11 and indicate that francium atoms, traveling at 600 m/s with divergences to 0.075 radians and possibly higher, can be cooled and transported to a slower provided sufficient laser power is available and the slower has a large diameter. And with a little ingenuity it should be possible to extend the transverse velocity acceptance even further. Section 10.2.3 describes the use of focusing and transverse laser cooling to reduce the francium beam's large normalized emittance after slowing. It works best when the atoms all have the same longitudinal velocity, but a less elegant version could be used to reduce the transverse size of the francium beam after transverse cooling.

10.4 Zeeman Slower

The deceleration of a francium atom by a laser in

the Zeeman slower, (where the Doppler shift of the oncoming atoms is balanced by a changing magnetic field to keep the laser in resonance) is given by

$$a = \frac{\hbar k \Gamma}{2m} \frac{s}{1 + s + [2(kv - \mu' B(z)/\hbar + \Delta/\Gamma)]^2}, \quad (10.8)$$

which is just Eq. 10.5 with the Doppler shift balanced by an added term $\mu' B(z)/\hbar$ for the Zeeman shift, where $B(z)$ is the magnetic field as a function of distance along the beam trajectory, and to a good approximation

$$\mu' = \mu_B [m_{J'} g_{J'} - m_J g_J]. \quad (10.9)$$

Here μ_B is the Bohr magneton, $m_{J'} = -3/2$ and $m_J = -1/2$ are the magnetic quantum numbers for the $7P_{3/2}$ and $7S_{1/2}$ states, respectively, and $g_{J'} = 4/3$ and $g_J = 2$ are the Landé g factors for the $7P_{3/2}$ and $7S_{1/2}$ states, respectively, and

$$g_J \approx 1 + \frac{J(J+1) + S(S+1) - L(L+1)}{2J(J+1)}. \quad (10.10)$$

Here $S = 1/2$ is the electron spin and L is the orbital angular momentum. The strong magnetic field approximation has been used because, for the $7P_{3/2}$ state, the interaction energy in the strong magnetic fields exceeds the hyperfine splitting; and in the ground state (which has a 43.57 GHz hyperfine splitting) the difference from the Breit-Rabi formula is less than one percent. Likewise, the nuclear magnetic moment has been neglected.

The maximum acceleration for ^{211}Fr that is achieved for a saturation factor of $s = 4.0$ is $-5 \times 10^4 \text{ m s}^{-2}$. To maintain phase stability, the magnetic field should change more slowly with downstream position than would be possible with the maximum deceleration (in other words less deceleration).

We adopt a deceleration of 80% of maximum, or $-4 \times 10^4 \text{ m s}^{-2}$. To slow a 600 m/s atom of ^{211}Fr to 60 m/s then takes 13.5 ms and the atoms travels $d_{||} = v_{||0} t - 1/2 a t^2 = 4.50 \text{ m}$ (Fig. 10.12). This is longer than most (maybe all) of the previously built Zeeman slowers; however they were not trying to slow atomic mass 211 from 600 m/s with high efficiency.

The maximum magnetic field needed is 0.37 T. A

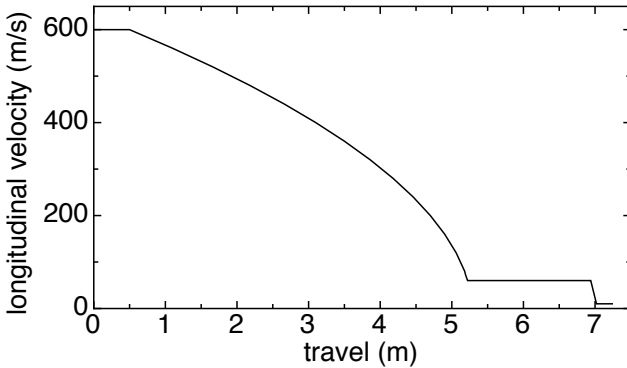


Figure 10.12: Longitudinal velocity as a function of travel distance. The atoms are slowed to 60 m/s then focused and transversely cooled before being slowed to 10 m/s. The first 0.5 m is used for transverse cooling. The beam optics are discussed in Section 10.5.

small bias magnetic field may also be added to avoid level crossings at low magnetic fields. This would bring the total to about 0.40 T. There is a well known problem in exiting the Zeeman slower at low velocity and low fields [MvdS99d]: the deceleration can continue in the magnetic fringe field. The solution to this problem is to put the low magnetic field end of the slower at the beginning where fast atoms enter and allow the slow atoms to exit from the high magnetic field. This then requires using atomic transitions whose transition energy decreases with increasing magnetic field [BDSRL91], which is to say σ^- transitions from $6S_{1/2} F = 5, M = -5 \leftrightarrow 6P_{3/2} F = 6, M = -6$.

A particularly attractive slower design is that of Cheiney et al. [CCBB⁺11b, CCBB⁺11a] which uses permanent magnets in a Halbach configuration [Hal80]. In addition to not needing electrical power or cooling, the magnets can be disassembled for vacuum system baking, and modified for small design changes. Their design allows access to the beam along their length, and if and when the beam-line becomes contaminated with long-lived francium daughters, the beam pipe can be replaced at small cost. The applied magnetic field however is transverse to the beam motion and will require that there

be an additional laser beam for repumping.

10.5 Zeeman Slower Beam Optics

Beam Divergence After Slowing

After a 0.5 m section of transverse cooling (Section 10.3), a very low divergence francium beam with a half-width of about 5 mm and velocities of up to 600 m/s enters the first of two Zeeman slowers (See Introduction Section 10.1). The first slower decelerates the atoms to about 60 m/s.

The slowing of the francium beam to 60 m/s from as high as 600 m/s causes an up to a factor of ten increase in beam divergence. There is also an increase in beam divergence and beam half-width due to transverse heating of the beam as it is slowed. In Section 10.3 and Eq. 10.6 it was found that the residual transverse velocity (a balance between cooling and heating) would be about ± 0.1 m/s. Transverse heating during the slowing of the francium atoms has no compensating cooling in this design and is thus given [MvdS99e] by

$$v_{\perp}(t) = \frac{\hbar k}{M} \sqrt{\Gamma t}, \quad (10.11)$$

where v_{\perp} is the transverse velocity acquired, t is time, and Γt is the total number of photons scattered. Because each photon transfers momentum resulting in a longitudinal velocity change $v = \hbar k/M = 2.6$ mm/s, the number of photons needed to slow the francium from 600 m/s is $\Gamma t = 600N/\hbar k = 2.3 \times 10^5$. Equation 10.11 then becomes

$$v_{\perp} = \sqrt{\frac{600\hbar k}{M}} = 1.25 \text{ m/s}. \quad (10.12)$$

The fastest francium atoms, initially at 600 m/s, absorb the greatest number of photons as they slow to 60 m/s and will acquire a transverse velocity $v_{\perp} = 1.25$ m/s. Francium atoms initially

at lower longitudinal velocities will suffer a bit less transverse heating.

At high longitudinal velocities, this transverse velocity is insignificant, but at 60 m/s it produces a divergence as large as 0.021 radians (including the 0.1 m/s after the initial transverse cooling section (Fig. 10.14)). And if nothing is done, the further increase in divergence and increase in beam size after further slowing makes capture into a magneto-optic trap problematic.

Longitudinal acceptance of the MOT

Because of francium's high mass, it decelerates slowly and will need a lower velocity than lighter alkalis to be captured into a MOT. In Sections 11.4.3 and 11.4.4 of Metcalf and van der Straten [MvdS99a], it is shown how, with sufficient laser beam size and power, high velocities can be captured into a MOT: Gibble, Kasapi, and Chu [GKC92] have captured 35 m/s cesium into a MOT with high efficiency.

However it is worth examining the possibility of slowing the francium to quite low velocities, both as a matter of demonstrating feasibility and because there are likely advantages in using a more modestly designed MOT. Lindquist, Stephens, and Wieman [LSW92] have examined MOT capture velocities for cesium for different laser power and laser beam sizes. Velocities of 15 m/s are found to be easy to capture, suggesting that ^{211}Fr would capture efficiently at 10 m/s. As a matter of accelerator physics, given sufficient cooling and focusing, the slowed francium beam can be matched to almost any MOT acceptance.

Transverse cooling of francium at a focus

To reduce the beam emittance we need to dissipatively cool the francium beam. This can be done at the exit of the first slower section, but if the beam is also brought to a focus, the transverse velocity is made high and cooling results in a greater reduction in phase space. Forming a focus would be difficult

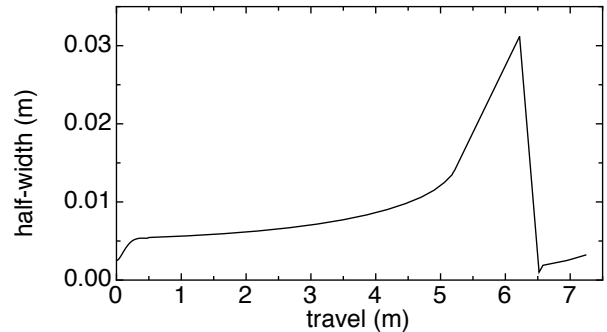


Figure 10.13: Francium beam half-width as a function of beam travel. The large increase in half-width is in the drift region upstream of the focusing element which then reduces the half-width while increasing the divergence. Due to the focusing and second stage of transverse cooling, the 10 m/s francium beam is narrow enough to go directly into a MOT.

before the francium beam is slowed, where the different initial velocities have different focal lengths. But once the beam has been slowed below 100 m/s, then 99% of the atoms are at nearly the same longitudinal velocity (Fig. 10.5) and so will have the same focal length.

Because the force applied by the magnetic sextupole focusing element is proportional to the atom's displacement, not its velocity, the atoms first travel through a drift space allowing the atoms with the largest transverse velocities to reach the largest displacements. Specifically the ± 0.021 radian francium beam is allowed to drift for 0.5 m, increasing its size from ± 2.1 cm to ± 3.3 cm (Fig. 10.13). This ensures that the atoms with the largest transverse velocity have the largest transverse displacement at the lens location.

At the end of the drift space, the beam is focused by a magnetic sextupole lens² (such as the ones used by Kaenders et al. [KLM⁺05] and Chaustowski, Leung, and Baldwin [R. 07]) with a focal length of 0.3 m. At the focus, the maximum transverse velocity will

²This will be similar to the magnetic sextupole lens used in the fountains (Section 3.12). A 2D MOT as described by Melentiev et al. [MBR⁺06] and others [Hoo93, HDV⁺96, LSHM99, SVH05]. may provide stronger focusing but the magnetic sextupole appears adequate for our use and seems simpler to operate.

be 6.5 m/s, and the focus size, by conservation of phase space, 4.8 mm. At the focus, the atoms are laser cooled in both transverse directions to a residual velocity of 0.1 m/s. And because the atoms are moving longitudinally at only 60 m/s, the cooling region is only 10 cm long for a maximum transverse acceleration of 2×10^4 m/s².

The force on a paramagnetic low-field-seeking atom [KLM⁺05] is given by

$$F = -\mu_B(\partial^2 B / \partial \rho^2)\rho, \quad (10.13)$$

where $\mu_B = 927 \times 10^{-26}$ J/T is the Bohr magneton and $\partial^2 B / \partial \rho^2$ is the radial second derivative of the magnetic field in the sextupole.

The linear increase in the force with radius provides for an analogy with conventional light optics,

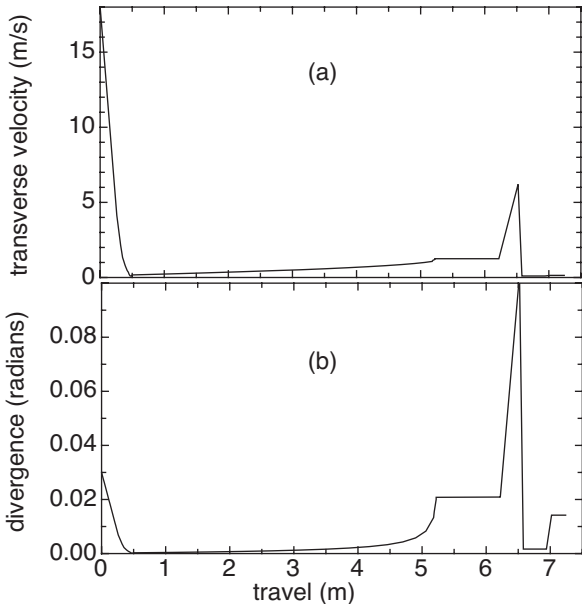


Figure 10.14: Francium beam transverse velocity (a) and divergence (ratio of the magnitude of the transverse velocity to longitudinal velocity) (b) as a function of travel. The initial decrease in transverse velocity and divergence is due to transverse cooling. The transverse velocity and divergence then increases in the slower due to beam heating and the divergence also increases due to reduced longitudinal velocity until it exits the first slower section at 60 m/s. Following a drift section, the beam is focused (sharp rise in transverse velocity and divergence) and then cooled at the focus. The atoms are then further slowed to 10 m/s.

so that the focal length of the lens is given by

$$f = \frac{Mv^2}{\mu_B(\partial^2 B / \partial \rho^2)L}, \quad (10.14)$$

where M is the mass of ²¹¹Fr, v its velocity and L the length of the magnet. For an ideal sextupole, the second derivative is given by

$$\frac{\partial^2 B}{\partial r^2} = 2B/r^2. \quad (10.15)$$

If we are looking for a focal length of about 0.3 m for francium at 60 m/s, an $L = 6$ cm lens must have a second derivative of the magnetic field equal to about 0.76 T/cm². Given a lens diameter of about 3 cm, and a remnant field approaching 1 T, this is easily achieved.

Second Slowing Section

Slowing the francium beam from 60 m/s to 10 m/s increases the transverse velocity to ± 0.14 m/s and the divergence to 0.014 radians, which is less than one degree. The beam half width is about ± 3 mm, adequate for being captured by a MOT. The transverse velocity and divergence of the francium beam, from the orthotropic oven (starting at 0.030 radian divergence) to the MOT is shown in Fig. 10.14.

Because the atoms are moving slowly, spending a long time in the laser beam, a deceleration of 2×10^4 m s⁻² results in a slower only about 10 cm long. To reduce end effects, it will be necessary to reduce the deceleration and make the slower section considerably longer.

Small bends in the beamline, one between the first and second slowing sections and one between the second slowing section and the MOT, may be needed. A small bend between the first and second deceleration sections will keep the laser beams from one slower section from interfering with atoms in the other section. Placed at the 60 m/s point, the bend, created by a magnetic lens, would not be difficult to put in. Likewise a small bend just upstream of the MOT can eliminate the need to shine a slowing laser beam through the MOT.

10.6 Orthotropic Oven and Zeeman Slower Prototypes

The orthotropic oven and especially the Zeeman slower can be prototyped using a stable alkali such as rubidium (Section 7.4). The orthotropic oven may initially be most easily prototyped using a weak ^{225}Ac source to produce ^{221}Fr . The ^{221}Fr daughters are short-lived so contamination is a minor issue. And the radioactivity makes it possible to obtain accurate measures of the number of atoms introduced into the oven and the number emitted.

The major development items are the transverse cooling and focusing, but the major design and cost item (not counting lasers) is the first stage Zeeman slower. Therefore a prototype slower can be designed using a laser chirp system in which the laser wavelength is scanned to keep the slowing atoms in resonance. This technique was used before Zeeman slowers became ubiquitous and while it has a low duty cycle, that is not a concern for a prototype.

Even without a first stage slower, the focusing section, bends, and the second stage slower (which is short and inexpensive to build) can be tested using a beam of slow stable alkali atoms filtered from a thermal beam using a magnetic gradient separator similar to the one developed by Ghaffari et al. [GGM⁺99].